Cartilage-on-a-chip with magneto-mechanical transformation for osteoarthritis recruitment

Hao Liu [a], Xiangyi Wu [b], Rui Liu [b], Weijun Wang [a,**], Dagan Zhang [a,***], Qing Jiang [a,*]

[a] *State Key Laboratory of Pharmaceutical Biotechnology, Department of Sports Medicine and Adult Reconstructive Surgery, Nanjing Drum Tower Hospital, The Affiliated Hospital of Nanjing University Medical School, 321 Zhongshan Road, Nanjing, 210008, Jiangsu, China*
[b] *Department of Rheumatology and Immunology, Institute of Translational Medicine, The Affiliated Drum Tower Hospital of Nanjing University Medical School, Nanjing, 210008, China*

A B S T R A C T

Osteoarthritis (OA) is a prevalent joint disease primarily induced by overstrain, leading to disability and significantly impacting patients' quality of life. However, current OA studies lack an ideal *in vitro* model, which can recapitulate the high peripheral strain of the joint and precisely model the disease onset process. In this paper, we propose a novel cartilage-on-a-chip platform that incorporates a biohybrid hydrogel comprising Neodymium (NdFeB)/Poly-GelMA-HAMA remote magneto-control hydrogel film. This platform facilitates chondrocyte culture and stress loading, enabling the investigation of chondrocytes under various stress stimuli. The Neodymium (NdFeB)/Poly-GelMA-HAMA hydrogel film exhibits magneto-responsive shape-transition behavior, further dragging the chondrocytes cultured in hydrogels under magnetic stimulation. It was investigated that inflammation-related genes and proteins in chondrocytes are changed with mechanical stress stimulation in the cartilage-on-a-chip. Especially, MMP-13 and the proportion of collagen secretion are upregulated, showing a phenotype similar to that of real human osteoarthritis. Therefore, we believed that this cartilage-on-a-chip platform provides a desired *in vitro* model for osteoarthritis, which is of great significance in disease research and drug development.

1. Introduction

Osteoarthritis (OA) is a degenerative joint disease and stands as the most prevalent cause of physical disability. The primary factor contributing to most OA cases is prolonged and excessive mechanical stress on the knee joint [1,2]. However, in the field of basic OA research, the commonly employed modeling method revolves around stimulating cells with inflammatory factors like IL-1β, while stress-related changes are often overlooked as influencing factors [3–5]. Consequently, there is an urgent need to develop a simulation model that places emphasis on stress changes within the articular cartilage microenvironment. Benefit from the rapid advancements a micro and nano manufacturing technology, a plethora of bionic 3D cultures, such as organ chips or organoids, have emerged [6–8]. Numerous experiments have demonstrated the significant potential of these techniques in recreating disease characteristics [9–13]. Nevertheless, most studies remain confined to static models, failing to adequately capture the dynamic evolution process of OA [13]. Therefore, a new dynamic 3D model that can achieve a more realistic simulation of the actual pathological process of OA needs to be developed.

In this study, inspired by the reciprocating motion of the human joint site, we have developed a novel biomimetic cartilage-on-a-chip system by incorporating magnetic response hydrogel into a microfluidic setup, as depicted in Fig. 1. The Organ chip (OC) system allows for the replication of organ microfluidic conditions *in vitro*, encompassing complex tissue interfaces, mechanical stress, fluid shear forces, and concentration gradients within the cell microenvironment [10,12,14–20]. However, the integration of periodic mechanical stress into organ chips for studying osteoarthritis (OA) is limited by existing material and structural constraints. Nowadays, magnetic hydrogels have emerged as an

---

ideal platform for mechanical simulation, as they can be remotely driven by externally applied magnetic fields. Their excellent magnetically-responsive deformation properties have found wide application in robot manufacturing, tissue engineering, and drug delivery [21–25]. Therefore, the integration of magnetic hydrogels and organ chips holds the promising potential to faithfully replicate motion patterns observed in OA pathogenesis.

Herein, we present a novel cartilage-on-a-chip integrated with magnetic hydrogel, offering a controllable and periodic stress regulation feature to simulate OA (Fig. 1a) [26]. To achieve this, we incorporated NdFeB powder with strong magnetism into GelMA-HAMA hydrogels to generate the magnetic hydrogel, which was engineered into perichondral layers at a physiological scale [27]. By introducing a circulating magnetic field, human chondrocytes cultured on the surface of the magnetic hydrogel experience cyclic stress. This traction process includes deformation in various directions during each cycle, closely mimicking the complex environment of the cartilage layer during joint movement. It was demonstrated that chondrocytes produce abnormal matrix remodeling under hyper-physiological mechanical stress, including secreting inflammatory factors such as MMP-13 and ADMTS-5, and the secretion of heterogeneous collagen with the decrease of collagen II and the increase of collagen I and collagen X [28–30]. Cell apoptosis was also observed [1,2,5]. Thus, this cartilage-on-a-chip featured magneto-mechanical transformation holds great promise as an ideal OA model for disease research and drug development.

2. Results and discussion

In a standard experimental setup, we integrated the GelMA-HAMA remote magneto-control hydrogel film to establish the cartilage-on-a-chip made by polydimethylsiloxane (PDMS) using microengineering technology. The microfluidics used bifurcated injection channels to convey culture medium, drugs or stimulation factors like cytokines. The magnetic hydrogel is first prepared into a dumbbell shape and then integrated into a flexible PDMS-based layered microchannel chip. In this cartilage chip, microfluidics involves layered perfusion channels, allowing for uniform perfusion of chondrocytes and culture medium. Thanks to the flexibility of the magnetic hydrogel, the layered chondrocytes exhibit anisotropic movement under a changing magnetic field. The changing magnetic field allows the magnetic hydrogel film to move controllably. We can control the desired mechanical loading on the film and the chondrocytes on it by controlling the magnetic field. As expected, the magnetic stimulation led to the movement of the NdFeB side of hydrogel, pulling the whole film. Meanwhile, the cells on the hydrogel films were also stretched, and this process is presented using fluorescent staining of phalloidin (Fig. 1b). By controlling the magnetic source, the mechanical loading can be adjusted to proper frequency, intensity, and
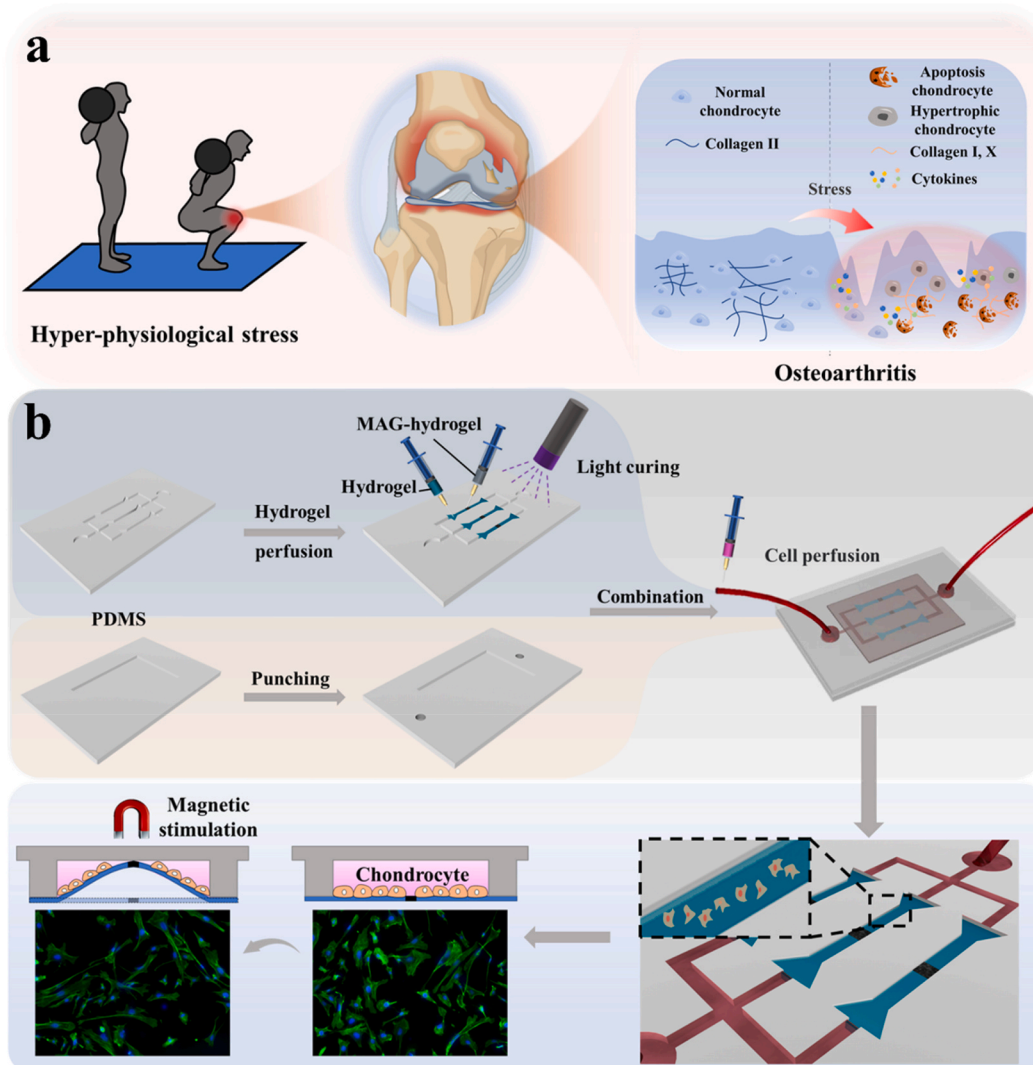

Fig. 1. (a) Schematic diagram of inflammatory changes in the knee joint under hyper-physiological stress; (b) Processes of chip assembly and cell perfusion.

duration. Thus, the platform was established.

We first confirmed the composition of the hydrogel. Gelatin methacryloyl (GelMA) and hyaluronic acid methacryloyl (HAMA) are both derived from chemically modified macromolecules widely distributed in organisms and have been extensively reported for bone tissue-related research. Previous studies have demonstrated that mixing GelMA and HAMA can simulate the mechanical strength and biocompatibility required for cartilage tissue [31–38]. Therefore, we introduce this combination to mimic cartilage tissue. Methacrylic anhydride was added to gelatin and hyaluronic acid solution drop by drop and dialysis was performed to obtain GelMA and HAMA. The curing can be completed in about 10 s with the addition of the photo-initiator LAP under 365 nm UV light (Fig. 2a) [39]. We have set different GelMA-HAMA concentration ratios to explore the optimal ratio, including 10:1, 10:2, and 10:3. After testing, the 10:2 hybrid hydrogel conveys appropriate elasticity and strength, and shows excellent biocompatibility. We verified the photocuring performance of the hydrogel and observed that it solidifies after 10 s of UV irradiation. Furthermore, the addition of high-density NdFeB powder does not affect the curing performance (Fig. S1). By combining different mask patterns, we can achieve the desired pattern (Fig. 2b). After UV curing, we prepared the magnetic hydrogel into the shape of a dragonfly, with densely stacked magnetic powder in its wings. The wings of the dragonfly can flap when exposed to a magnetic field generated by a magnet (Fig. 2c). Furthermore, to investigate the 3D microstructure of the hydrogels, scanning electron microscopy (SEM) was applied to show the freeze-dried GelMA-HAMA hydrogel and the NdFeB/GelMA-HAMA hydrogel (Fig. 2d). When the hydrogel is integrated into the chip, an appropriate shape is necessary. In order to fix the hydrogel in the tank, the dumbbell shape was chosen, where the protrusion at both ends of the hydrogel is restricted to move in the radial and normal directions, thus showing only elongation and no movement in the magnetic field. The system is prepared for integrated into the cartilage-on-a-chip.

The GelMA and HAMA hydrogel were preliminarily characterized by FTIR and 1Hnmr (Fig. 3a, b, S2). We then conducted mechanical performance tests on the magnetic hydrogel [40]. The experimental results indicated that as the concentration of HAMA increased, the hydrogel's Young's modulus increased, but the strain at the fracture limit decreased (Fig. 3c and f). When the GelMA-HAMA concentration ratio was 5:1, the hydrogel was subjected to different levels of tensile strain and ten cycles of stretching. The stress-strain curves showed a consistent trend, indicating that the hydrogel has stable fatigue resistance properties (Fig. 3d and e). The swelling ratio of each combination is also tested using weighing method (Fig. 3g). Also, the degradation test proves that the addition of HAMA helps resist the degradation by matrix-degrading enzyme (Fig. 3h) [22]. The results illustrate that a low HAMA concentration provides inadequate mechanical strength and anti-degradation, while the high concentration of HAMA shows weak magnetic response and a high swelling ratio. Therefore, the GelMA hydrogel with 5 % concentration and the HAMA hydrogel with 1 % concentration (GelMA: HAMA = 5:1) were proper for further experiment.

To validate the biocompatibility of the GelMA-HAMA hydrogel, we cultured the human chondrocyte cell line C28/I2 on it [41,42]. Benefit from the low toxicity, biological interaction, and biodegradability of the hydrogel, it presented a great affinity to the cells, shown by the fluorescent staining of phalloidin, dead/live staining and cck-8 test on day 1, day 3 and day 7 (Fig. 4a and b). As shown, the results of live/dead staining demonstrate that cells proliferate well when cultured on the hydrogel, similar to the results of culturing in a cell culture dish. The phalloidin staining shows that cells cultured on the hydrogel have fewer pseudopodia and exhibit a morphology more similar to that of chondrocytes in the body. Also, same test and cck-8 test have been performed to validate the biocompatibility of NdFeB-hybrid hydrogel (Fig. 4a and b, S3.) and the results showed no difference between the magneto-hydrogel and the pure hydrogel, indicating that the NdFeB-hybrid hydrogel has no or only a small amount of biological toxicity.

Furthermore, we tested the secretion-promoting ability of the hydrogel [43,44]. C28/I2 cells were cultured on the same area of cell culture plate (CCP) and hydrogel surface for 7 days, and immunofluorescence staining and quantitative analysis were carried out. The results showed that the cells growing on the hydrogel expressed more type I and type II collagen, and secreted a certain amount of matrix, and the subsequent immunofluorescence quantitative analysis visually displayed
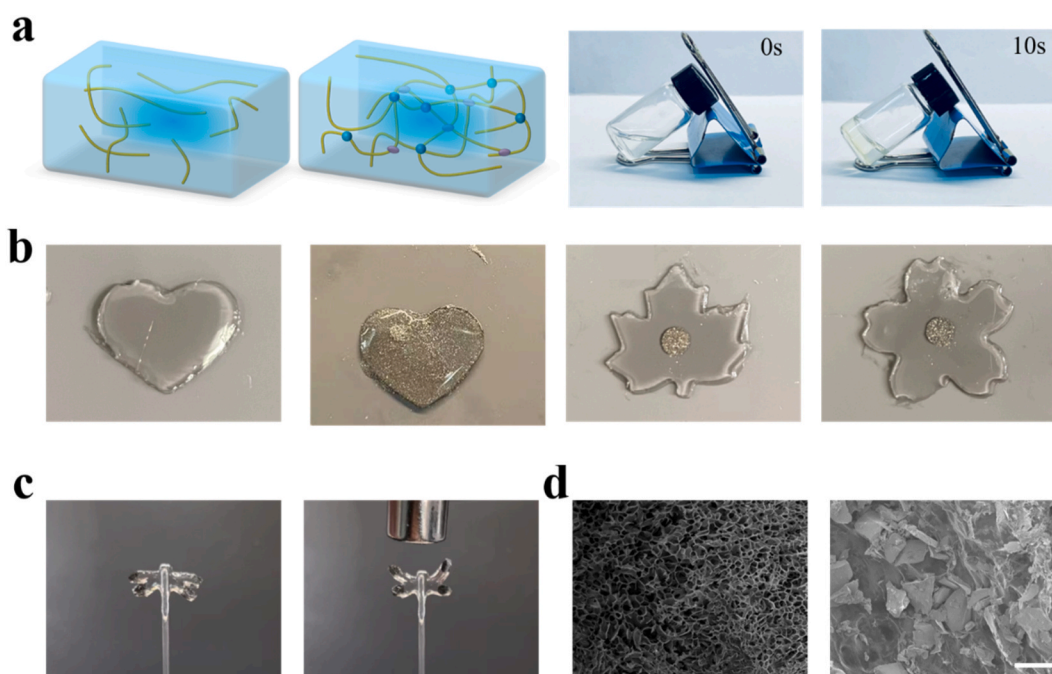
Fig. 2. (a) The GelMA-HAMA hydrogel is cured in 10s under 365 nm UV light. (b) Various kinds of shapes of the NdFeB-hybrid GelMA-HAMA hydrogel. (c) The wings of the dragonfly-like-hydrogel can flap when exposed to a magnetic field. (d) The SEM image of the pure hydrogel and the NdFeB-hybrid hydrogel. Scale bar, 50 μm.
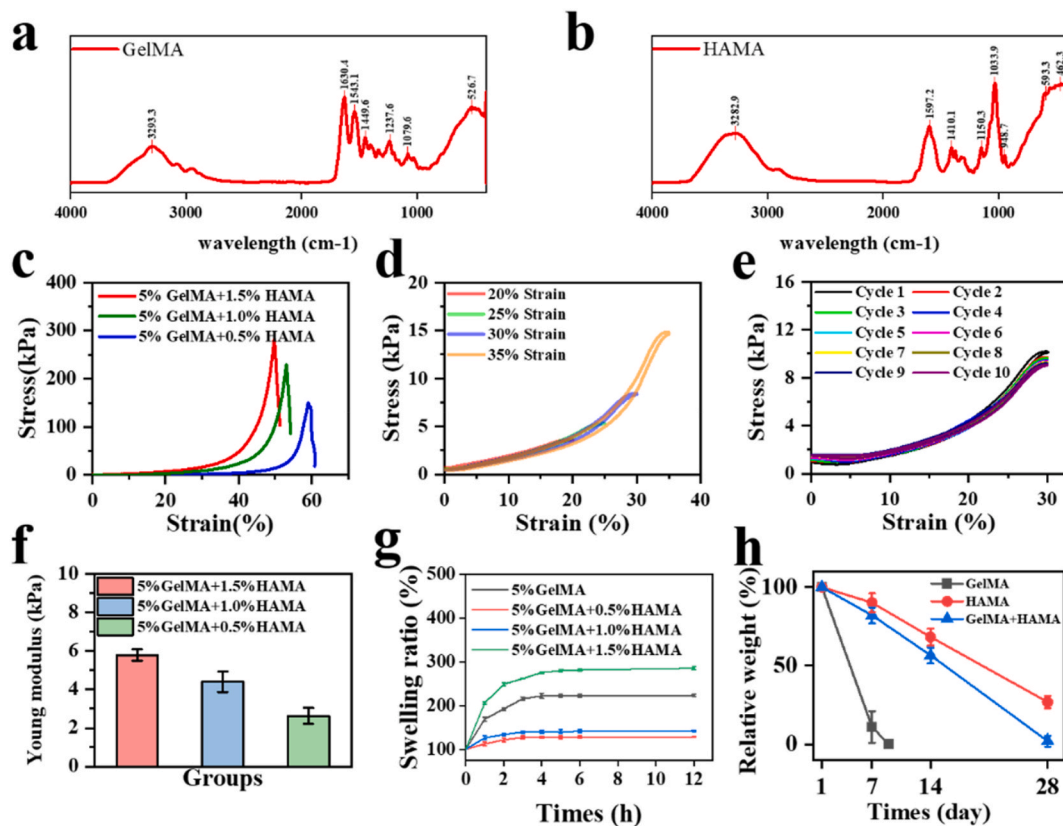
Fig. 3. (a,b) FTIR test of the GelMA and HAMA hydrogels. (c) The strain-stress image of the fracture limit of the hydrogel with different HAMA concentration. (d) The strain-stress image of different deformation of the hydrogel. (e) The strain-stress image of the hydrogel in 10 consecutive stretch cycling. (f) The Young modulus of the hydrogel with different HAMA concentration. n = 5. (g) The swelling ratio of the hydrogel with different HAMA concentration. n = 5. (h) The degradation rate of different hydrogels. n = 5.
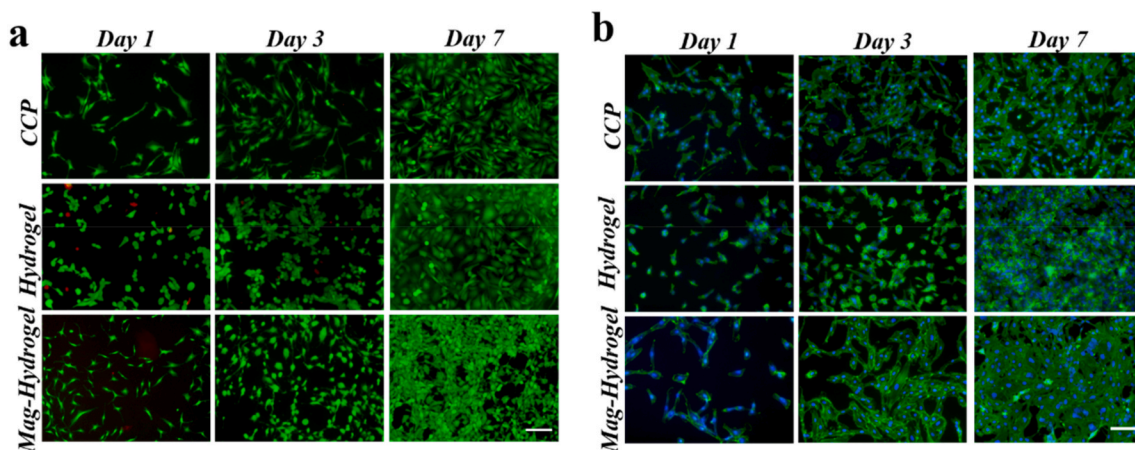

Fig. 4. (a) The dead-live image of cells cultured on the CCP, GelMA-HAMA hydrogel and NdFeB-GelMA-HAMA hydrogel for 1, 3, and 7 days. (b) The phalloidin staining of cells cultured on the CCP, GelMA-HAMA hydrogel and NdFeB-GelMA-HAMA hydrogel for 1, 3, and 7 days. Scale bar, 100 μm.

the results (Fig. 5a, b, 5c). The corresponding qPCR detection also showed that the hydrogel can promote the collagen secretion function of chondrocytes. (Fig. 5d and e).

To further confirm the establishment of the chip and the effectiveness of the OA model, we simulated the cartilage system. The magnetic hydrogel undergoes deformation of a certain intensity and frequency under the action of an external alternating magnetic field. First, the chondrocytes underwent 5 days of mechanical stimulation with different hydrogel deformation from 0 % to 30 %. The hydrogel was stimulated 4 h a day, with different groups including a control group, 10

% deformation group 20 % deformation group, and a 30 % deformation group. The frequency of dynamic magnetic fields is 0.5 Hz. After 5 days of stimulation, the chondrocytes were detected for qPCR assay (Fig. 6b). The results showed that the hyper-physiological mechanical loading could contribute the osteoarthritis of chondrocytes. When the deformation is limited under 10 %, the chondrocytes show no different from those cultured with no deformation. When the deformation is increased to 20 %–30 %, the chondrocytes showed increased osteoarthritis phenotype. Then, experiments based on different stimulation frequency from 0 Hz to 1 Hz were completed. Similar to before, chondrocytes
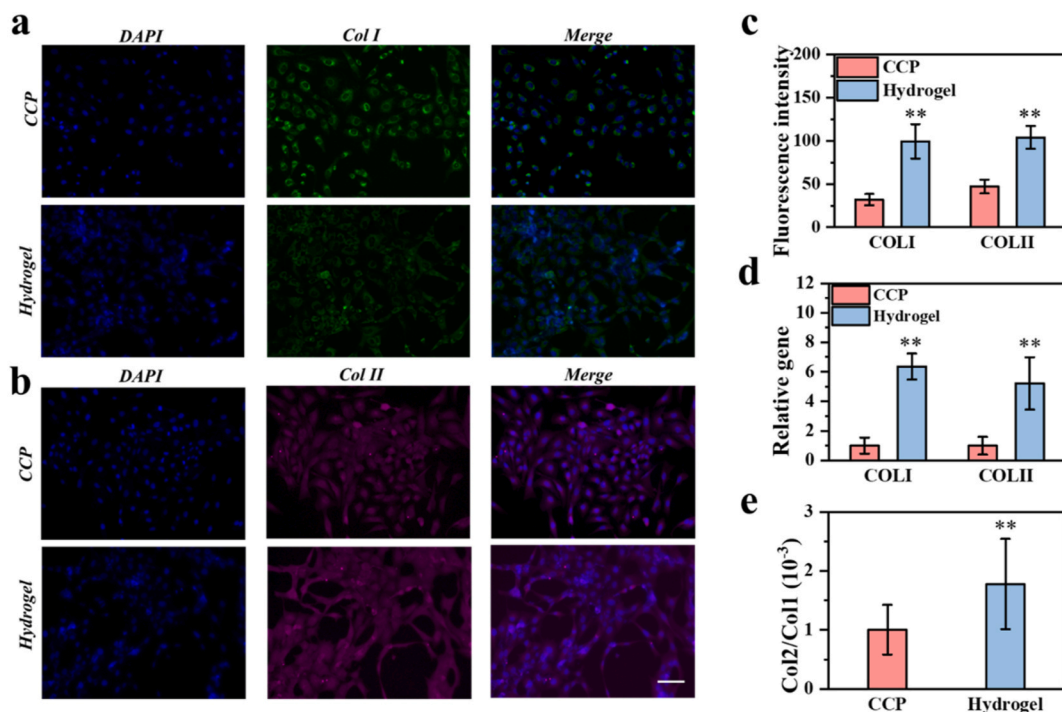
Fig. 5. (a, b) Fluorescence microscopy images of the cells stained for nuclei (blue), Collagen I (green) and Collagen II (purple). (c) The fluorescence quantitative analysis of the fluorescence microscopy images. (d) Relative expression of Col1A1 and Col2A1 of cells cultured on the culture dish and the hydrogel. n = 3. (e) Col2A1/Col1A1 expression ratio of cells cultured on the culture dish and the hydrogel. n = 3. *, p < 0.05, **, p < 0.01. Scale bar, 100 μm.
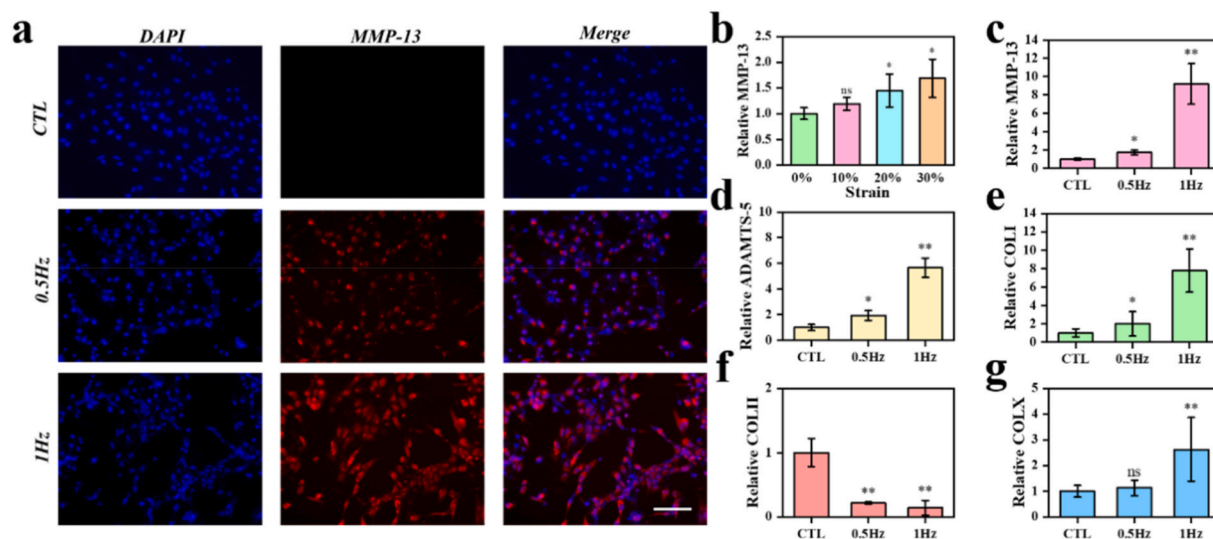
Fig. 6. (a) Fluorescence microscopy images of the cells stained for nuclei (blue) and MMP-13 (red) under different stimulate frequency. (b) Relative inflammation related genes expression of cells under increasing stimulation intensity. n = 3. (c,d) Relative inflammation related gene expression of cells under increasing stimulation frequency. n = 3. (e) Relative collagen related genes expression of cells under increasing stimulation frequency. n = 3. *, p < 0.05, **, p < 0.01. Scale bar, 100 μm.

represent obvious osteoarthritis phenotype as the increase of stimulation frequency (Fig. 6c and d). And the immunofluorescence staining is applied for localization and quantitative analysis of osteoarthritis related proteins. The results of cellular immunofluorescence showed that the expression level of matrix degrading protease MMP-13 secreted by chondrocytes increases under increasing frequency stimuli. The results of cellular immunofluorescence showed the expression level of matrix degrading protease MMP-13 produced by C28/I2 cells under different frequency stimuli (Fig. 6a). These results reveal that under specific stimulation intensity and frequency, chondrocytes cultured in

the cartilage-on-a-chip undergo changes similar to osteoarthritis, accompanied by increased production of matrix-degrading enzymes and abnormal collagen secretion. In order to further verify the superiority of this method over traditional methods, C28/I2 cells were cultured on hydrogels of the same shape and subjected to cytokine stimulation and mechanical stimulation (20 % deformation, 1 Hz) respectively. qPCR results showed that mechanically stimulated chondrocytes produced more inflammatory factors than those stimulated by cytokines (Fig. S4). With TUNEL assay, we detected the apoptosis level of the chondrocytes (Fig. S5). The qPCR experiments were repeated three times for each

group. The gene primers that were used are listed in Table 1.

3. Conclusion

In summary, we developed a microfluidic platform which can exert mechanical loading on chondrocytes by magneto-responsive shape-transition hydrogel. This innovative magnetic hydrogel undergoes transformation with magneto-stimulation, leading to displacement and effectively pulling the chondrocytes cultured on the hydrogel. In addition, we seamlessly integrated the hydrogel into the cartilage-on-a-chip system with microfluidics. This allowed us to precisely simulate the microenvironment experienced by articular cartilage under pressure, effectively accelerating the degeneration of chondrocytes and the progression of osteoarthritis. Notably, unlike other organ-on-a-chip, this chip platform enables easy control of the mechanical pressure, with adjustable intensity and frequency using an electromagnet. This cartilage-on-a-chip platform offers an exceptional mechanical loading method which can be remotely controlled, which is of great significance in osteoarthritis research and *in vitro* drug development. Therefore, we believe that the cartilage-on-a-chip platform based on magneto-responsive shape-transition NdFeB/GelMA-HAMA hydrogel holds immense potential for extensive application in the field of biomedical engineering.

4. Experimental section

Materials: GelMA, HAMA were self-prepared. TrypLE and DMEM were purchased from Gibco. PBS (phosphate-buffered saline) and DAPI (4′,6-diamidino-2-phenylindole) were obtained from Beyotime Biotechnology. Phalloidin stain and all antibodies were acquired from Abcolonal. Live/Dead kit were obtained from keygen biotech corporation. PDMS (SYLGARD 184) and its curing agent were acquired from Dow Corning Corporation. C28/I2 cell line was purchased from BLUE-FBIO. All reagents were used as received.

Preparation of the GelMA and HAMA hydrogel: 10 g of gelatin was added to 100 ml of PBS and stir at 50 °C for 3 h. After the gelatin is completely dissolved, adjust the pH of the solution to between 7 and 8, add 6 ml of MA drop by drop to the bottle, and stir at 50 °C for 3 h. The reacted solution is centrifuged and the unreacted MA is removed. The supernatant was diluted and poured into the dialysis bag, and dialysis was carried out in heated ddH₂O for 7 days. After dialysis, freeze-drying was performed to obtain GelMA. And HAMA was made by a similar method.

Preparation of the magnetic hydrogel: The GelMA and HAMA (the mass ratio of monomer GelMA and HAMA was 5:1) were mixed and dissolved in PBS as solution A. Then, the NdFeB (80 % w/v) was dispersed in the same solution as solution A, named solution B. The solution B was first exposed to UV light (365 nm, 10s) with a photo-initiator LAP (0.5 %, v/v) being added to form the magneto-hydrogel and these hydrogels were then cut into small fibro-like pieces for further utilization. The pregel solution A was composed of GelMA (5 wt%) and HAMA (1 wt%), a photo-initiator LAP (0.5 %, v/v) was added into the above suspensions. After extensive mixing, the pregel solution A was poured into the microfluidic channel with NdFeB hybrid films putting on the middle after which is exposed to UV light (365 nm, 10s). Finally, the

magnetically responsive hydrogel was prepared in dumbbell shape, 1 mm wide and 10 mm long, and the two ends of the hydrogel protrated as equilateral triangles with 3 mm side length.

Magneto-responsive behavior: The magnetic responsive phase transition of the GelMA-HAMA composite hydrogel was first investigated. By using a mask with a designed pattern, a dumbbell-shaped hydrogel membrane was fabricated after UV-induced polymerization of the GelMA-HAMA mixture solution. The membrane was then placed next to an electromagnet. After the stretching, the electromagnet was switched off to let the membrane return to the former shape under natural state. In order to regulate the interval, we add a pulse generator into the circuit.

Assembling Process of Microfluidic Chip: The microfluidic chip comprises an upper and lower part. Initially, PDMS was mixed with 1 % sylgard, stirred, and poured into the template. Subsequently, the template was subjected to vacuum treatment in a vato vacuum machine until no bubbles were observed in the liquid PDMS. Following this step, the template was placed in an oven for 8 h to allow complete solidification of the PDMS. Once solidified, the PDMS was separated from the template to obtain the upper half of the chip. The lower half consisted of dumbbell-shaped PDMS that matched the size of its counterpart above with the inner diameter of 1 mm wide and 10 mm long to hold the hydrogel made above. Finally, bonding occurred by pressing and assembling together both halves.

Characterization of swelling rate: Different composition of hydrogel was cured as several small pieces with same volumn. After light curing, the hydrogel was immediately weighed with the result being recorded as W_0. Then the hydrogel was put into PBS buffer for 24 h, and was weighed per 1 h as W, the swelling ratio is calculated according to the formula $ESR = \frac{W - W0}{W0}$.

Characterization of mechanical properties: The hydrogel solutions of different components are poured into the dumbbell shaped mold. The thinner part is 20 mm long, 2 mm wide and 1 mm high, respectively. The thicker part at both ends is fixed by the fixture of the biomechanical instrument, and their mechanical properties such as fracture limit and fatigue resistance are tested respectively. We determined the Young's modulus of GelMA-HAMA hydrogels with varying ratios by assessing their elastic stretch under external tensile stress and subsequently computed it using the formula: $E = \sigma/\varepsilon$, where E denotes Young's modulus, σ represents stress, and ε signifies elastic deformation.

Characterization of the degradation: First, several hydrogel cubes of the same size are made under 365 nm UV light, 10s, which are respectively composed of GelMA, HAMA and GelMA-HAMA. They were immersed in a solution containing type II collagenase and hyaluronidase, incubated at 37 °C for 28 days, freeze-dried and weighed every seven days. The enzyme activity of type II collagenase is 4u/ml, hyaluronidase concentration is 20 u/ml, the solution was changed every 3 days.

Cell Culture: After the hydrogel formation, it was illuminated with ultraviolet light for 3 h and washed three times with PBS. After integration into the PDMS chip, C28/I2 cells were added. The cell-laden NdFeB/GelMA-HAMA hydrogel was cultured statically in DMEM medium containing 10 % FBS and 1 % penicillin-streptomycin (37 °C, CO₂, 5 %) for 7 days for subsequent experiments.

Biocompatibility Assessment: The cell-laden hydrogels were cultured

Table 1
Primers for real-time PCR.

Gene	Forward primer (5′-3′)	Reverse primer (5′-3′)
GAPDH	CAATGACCCCTTCATTGACC	TTGATTTTGGAGGGATCTCG
Mmp-13	TTGAGCTGGACTCATTGTCG	GGAGCCTCTCAGTCATGGAG
ADAMTS-5	GGCCTCCATCGCCAATAGG	GGATAGCTGCATCGTAGTGCT
Col1a1	GAGGGCCAAGACGAAGACATC	CAGATCACGTCATCGCACAAC
Col2a1	GCTCCTCTTAGGGGCCACT	CCACGTCTCACCATTGGGG
Col10a1	TTCTGCTGCTAATGTTCTTGACC	GGGATGAAGTATTGTGTCTTGGG
IL-1β	ATGATGGCTTATTACAGTGGCAA	GTCGGAGATTCGTAGCTGGA

for 1, 3, and 7 days, followed by incubation with a live/dead staining reagent for 40 min. Subsequently, the samples were observed using fluorescence microscopy to acquire images. Similarly, the cell-laden hydrogels cultured for 1, 3, and 7 days were fixed in a solution of paraformaldehyde-PBS (4 % v/v) for 30 min and then permeabilized with Triton X-100-PBS (0.3 % v/v) for an additional 30 min. To visualize F-actin and cell nuclei, Alexa Fluor 488 Phalloidin (diluted at a ratio of 1:400) and DAPI (diluted at a ratio of 1:1000), respectively, were used to obtain fluorescence images of the samples.

Chondrogenic Function Evaluation: The hydrogels cultured for 7 days were retrieved and fixed in 4 % (v/v) paraformaldehyde-PBS solution for 30 min, followed by permeabilization with 0.3 % (v/v) Triton X-100-PBS solution for 30 min. Subsequently, the samples were incubated with primary antibodies against Collagen I and Collagen II for a duration of 10 h, followed by three washes with PBS. Following this, the samples were subjected to incubation with fluorescent secondary antibodies for an hour and visualized under a fluorescence microscope. Additionally, RNA was extracted from the cells cultured for 7 days post-digestion, and gene expression analysis was performed using qPCR.

Osteoarthritis Induction Assessment: When the cells reached approximately full confluency, cyclic stretching (0.5 or 1 Hz) was applied to the microdevice for 4 h per day over a period of 7 days. Subsequently, the stress-induced hydrogels were extracted and fixed in 4 % (v/v) paraformaldehyde-PBS for 30 min, followed by permeabilization with 0.3 % (v/v) Triton X-100-PBS for another 30 min. The samples were then subjected to a primary antibody incubation against MMP-13 for a duration of 10 h, followed by incubation with fluorescent secondary antibodies for an hour. Finally, fluorescence microscopy was employed to observe the samples. Additionally, qPCR analysis was conducted to assess matrix degradation ability and changes in collagen secretion types of inflammatory chondrocytes.

Apoptosis Detection: The stress-induced hydrogels were removed from culture and fixed in 4 % (v/v) paraformaldehyde-PBS solution for half an hour before being permeabilized using a solution containing 0.3 % (v/v) Triton X-100-PBS for another 30 min. TUNEL detection solution was added to the samples which were then incubated at a temperature of 37 °C in darkness for 60 min prior to microscopic examination aimed at detecting apoptotic cells.

Statistical analysis: The data were shown as mean ± standard deviation. Each independent test was repeated at least 3 times with parallel tests to ensure validity. Statistical analysis was performed using IBM SPSS Statistics 22. The statistical significance was set as *$p < 0.05$ and **$p < 0.01$.

CRediT authorship contribution statement

Hao Liu: Data curation, Formal analysis, Investigation, Methodology, Software, Writing – original draft. **Xiangyi Wu:** Data curation, Formal analysis, Methodology, Visualization, Writing – review & editing. **Rui Liu:** Methodology, Writing – review & editing. **Weijun Wang:** Project administration, Resources, Supervision. **Dagan Zhang:** Funding acquisition, Project administration, Resources, Supervision, Validation. **Qing Jiang:** Conceptualization, Funding acquisition, Project administration, Supervision.

Declaration of competing interest

The authors declare that they have no known competing financial interests or personal relationships that could have appeared to influence the work reported in this paper.

Acknowledgements

Appendix A. Supplementary data

Supplementary data to this article can be found online at https://doi.org/10.1016/j.bioactmat.2023.10.030.

References

[1] S. Glyn-Jones, et al., Osteoarthritis, Lancet 386 (9991) (2015) 376–387.
[2] J. Martel-Pelletier, et al., Osteoarthritis, Nat. Rev. Dis. Prim. 2 (2016), 16072.
[3] P.J. Cope, et al., Models of osteoarthritis: the good, the bad and the promising, Osteoarthritis Cartilage 27 (2) (2019) 230–239.
[4] T. Fang, et al., Molecular mechanisms of mechanical load-induced osteoarthritis, Int. Orthop. 45 (5) (2021) 1125–1136.
[5] M. Kapoor, et al., Role of proinflammatory cytokines in the pathophysiology of osteoarthritis, Nat. Rev. Rheumatol. 7 (1) (2011) 33–42.
[6] Y. Han, et al., Biomimetic injectable hydrogel microspheres with enhanced lubrication and controllable drug release for the treatment of osteoarthritis, Bioact. Mater. 6 (10) (2021) 3596–3607.
[7] Z. Wang, et al., Pharmaceutical electrospinning and 3D printing scaffold design for bone regeneration, Adv. Drug Deliv. Rev. 174 (2021) 504–534.
[8] Y. Lei, et al., Shear-responsive boundary-lubricated hydrogels attenuate osteoarthritis, Bioact. Mater. 16 (2022) 472–484.
[9] R. Gottardi, Load-induced osteoarthritis on a chip, Nat. Biomed. Eng. 3 (7) (2019) 502–503.
[10] L. Li, et al., Graphene hybrid anisotropic structural color film for cardiomyocytes' monitoring, Adv. Funct. Mater. 30 (3) (2019).
[11] P. Occhetta, et al., Hyperphysiological compression of articular cartilage induces an osteoarthritic phenotype in a cartilage-on-a-chip model, Nat. Biomed. Eng. 3 (7) (2019) 545–557.
[12] Y. Zhu, et al., A biomimetic human lung-on-a-chip with colorful display of microphysiological breath, Adv. Mater. 34 (13) (2022), e2108972.
[13] Y. Hu, et al., Bone/cartilage organoid on-chip: construction strategy and application, Bioact. Mater. 25 (2023) 29–41.
[14] Y. Zhu, et al., Engineering human brain assembloids by microfluidics, Adv. Mater. 35 (14) (2023), e2210083.
[15] Small, Zheng.pdf, 2016.
[16] C. Shao, et al., Droplet microfluidics-based biomedical microcarriers, Acta Biomater. 138 (2022) 21–33.
[17] C. Ma, et al., Organ-on-a-Chip: a new paradigm for drug development, Trends Pharmacol. Sci. 42 (2) (2021) 119–133.
[18] R.E. Young, D.D. Huh, Organ-on-a-chip technology for the study of the female reproductive system, Adv. Drug Deliv. Rev. 173 (2021) 461–478.
[19] D.E. Ingber, Human organs-on-chips for disease modelling, drug development and personalized medicine, Nat. Rev. Genet. 23 (8) (2022) 467–491.
[20] G. Saorin, I. Caligiuri, F. Rizzolio, Microfluidic organoids-on-a-chip: the future of human models, Semin. Cell Dev. Biol. 144 (2023) 41–54.
[21] X. Liu, et al., Magnetic living hydrogels for intestinal localization, retention, and diagnosis, Adv. Funct. Mater. 31 (27) (2021).
[22] A. Pardo, et al., Magnetic nanocomposite hydrogels for tissue engineering: design concepts and remote actuation strategies to control cell fate, ACS Nano 15 (1) (2021) 175–209.
[23] X. Zhang, et al., Magneto-responsive microneedle robots for intestinal macromolecule delivery, Adv. Mater. 33 (44) (2021), e2104932.
[24] Y. Dong, A.N. Ramey-Ward, K. Salaita, Programmable mechanically active hydrogel-based materials, Adv. Mater. 33 (46) (2021), e2006600.
[25] A.G. Kurian, et al., Multifunctional GelMA platforms with nanomaterials for advanced tissue therapeutics, Bioact. Mater. 8 (2022) 267–295.
[26] J. Sun, et al., "Slow walk" mimetic tensile loading maintains human meniscus tissue resident progenitor cells homeostasis in photocrosslinked gelatin hydrogel, Bioact. Mater. 25 (2023) 256–272.
[27] S. Hu, et al., Cellulose hydrogel-based biodegradable and recyclable magnetoelectric composites for electromechanical conversion, Carbohydr. Polym. 298 (2022), 120115.
[28] T. Hodgkinson, et al., Mechanosignalling in cartilage: an emerging target for the treatment of osteoarthritis, Nat. Rev. Rheumatol. 18 (2) (2022) 67–84.
[29] F. Motta, et al., Inflammaging and osteoarthritis, Clin. Rev. Allergy Immunol. 64 (2) (2022) 222–238.
[30] Q. Yao, et al., Osteoarthritis: pathogenic signaling pathways and therapeutic targets, Signal Transduct. Targeted Ther. 8 (1) (2023) 56.
[31] L. Han, et al., Biohybrid methacrylated gelatin/polyacrylamide hydrogels for cartilage repair, J. Mater. Chem. B 5 (4) (2017) 731–741.

[32] S. Xiao, et al., Gelatin methacrylate (GelMA)-Based hydrogels for cell transplantation: an effective strategy for tissue engineering, Stem Cell Rev Rep 15 (5) (2019) 664–679.

[33] H. Hu, et al., miR-23a-3p-abundant small extracellular vesicles released from Gelma/nanoclay hydrogel for cartilage regeneration, J. Extracell. Vesicles 9 (1) (2020), 1778883.

[34] Y. Fan, et al., Hybrid printing using cellulose nanocrystals reinforced GelMA/HAMA hydrogels for improved structural integration, Adv. Healthcare Mater. 9 (24) (2020), e2001410.

[35] K. Ma, et al., Application of robotic-assisted in situ 3D printing in cartilage regeneration with HAMA hydrogel: an in vivo study, J. Adv. Res. 23 (2020) 123–132.

[36] G. Wang, et al., Chondrocyte spheroids laden in GelMA/HAMA hybrid hydrogel for tissue-engineered cartilage with enhanced proliferation, better phenotype maintenance, and natural morphological structure, Gels 7 (4) (2021).

[37] L. Jia, et al., Bioprinting and regeneration of auricular cartilage using a bioactive bioink based on microporous photocrosslinkable acellular cartilage matrix, Bioact. Mater. 16 (2022) 66–81.

[38] C. Zhou, et al., Hydrogel platform with tunable stiffness based on magnetic nanoparticles cross-linked GelMA for cartilage regeneration and its intrinsic biomechanism, Bioact. Mater. 25 (2023) 615–628.

[39] F. Zhou, et al., Rapid printing of bio-inspired 3D tissue constructs for skin regeneration, Biomaterials 258 (2020), 120287.

[40] G. Wang, et al., Bio-based hydrogel transducer for measuring human motion with stable adhesion and ultrahigh toughness, ACS Appl. Mater. Interfaces 13 (20) (2021) 24173–24182.

[41] X. Li, et al., 3D culture of chondrocytes in gelatin hydrogels with different stiffness, Polymers 8 (8) (2016).

[42] Z. Jian, et al., 3D bioprinting of a biomimetic meniscal scaffold for application in tissue engineering, Bioact. Mater. 6 (6) (2021) 1711–1726.

[43] Z. Qiao, et al., Bioinspired stratified electrowritten fiber-reinforced hydrogel constructs with layer-specific induction capacity for functional osteochondral regeneration, Biomaterials 266 (2021), 120385.

[44] B. Huang, et al., Hydrogel composite scaffolds achieve recruitment and chondrogenesis in cartilage tissue engineering applications, J. Nanobiotechnol. 20 (1) (2022) 25.